Transactions of the **14th International Conference on Structural Mechanics in Reactor Technology** (SMiRT 14), Lyon, France, August 17-22, 1997 **K06/6**

Study on the energy dissipated by structure in turbine building

Watanabe S., Kageyama H., Ichikawa K., Kanaya M.
Tokyo Electric Power Services Co., Japan

ABSTRACT : It is important to investigate the damage of the structure. The energy dissipated by the structure in the turbine building of an ABWR type nuclear power plant during earthquake is investigated. One artificial wave and two observed strong ground motions are used in the inelastic response analyses. The hysteresis model is considered as the most dominant factor. It is concluded that the ductility factor has a close relationship with hysteresis energy corresponding to the specified hysteresis characteristics.

1. INTRODUCTION

Inelastic behavior of the structure members in the turbine building of an ABWR type nuclear power plant during earthquake is discussed here. The basement and the ground floor consist of reinforced concrete shear walls that are designed by the allowable stress method. On the other hand, the operating floor consists of the moment resisting frames. Because the frame structure will be designed by the ultimate strength design method in the future, it becomes necessary to investigate inelastic behavior of the turbine building. Energy dissipation of the system under earthquake loading has been a topic of interest for these years. In this study the inelastic response analyses of the structure members are performed and damage of the structure by energy dissipation during strong ground motion is estimated.

2. ANALYTICAL CONDITION

2.1 *Energy Response*

The equation of motion for a single degree of freedom system subjected to a ground motion is given by:

$$m\ddot{x} + c\dot{x} + F(x) = -m\ddot{y}_0 \qquad (1)$$

where $F(x), \ddot{x}, \dot{x}, \ddot{y}_0$ are the restoring force of the system, relative acceleration, relative velocity to the ground and ground acceleration, respectively. Mass m and damping coefficient c are constant in the system. $F(x)$ is given by the inelastic load–deformation characteristics specified in analysis. The equilibrium of energies of the system[1] are described as follows:

$$E_V + E_D + E_H = E_I \tag{2}$$

here E_V, E_D, E_H and E_I represent the energies dissipated by the system due to the inertia, damping and hysteresis and input energy, respectively. Equation (2) may be expressed as:

$$\int_0^T m\ddot{x}\dot{x}dt + \int_0^T c\dot{x}\dot{x}dt + \int_0^T F(x)\dot{x}dt = -\int_0^T m\ddot{y}_0\dot{x}dt \tag{3}$$

in which T is duration time of strong motion. The structure will dissipate input energy of earthquake as hysteresis energy and damping energy. Damaging potential of earthquake to the structure will be estimated by energy E_H. Inelastic responses are obtained for specified level of ductility factors μ given as the following equation.

$$\mu = \delta / \delta_y \tag{4}$$

δ is maximum response displacement and δ_y is yield displacement. Damage of the structure can be estimated by energy factor μ_e that is defined as follows.

$$\mu_e = E_H / F_y \delta_y \tag{5}$$

here, F_y and δ_y are yield force and yield displacement, respectively. To discuss the inelastic behavior, momentary input energy(ΔE) [2] is derived from the following equation.

$$\Delta E = -\int_t^{t+\Delta t} m\ddot{y}_0\dot{x}dt \tag{6}$$

where Δt is the time for half cycle of energy response due to inertia and input energies $(E_I - E_V)$, but is not constant during earthquake.

2.2 *Analytical Model*

In this study two types of the structure members with quite short period system are analyzed. One is crane column of the operating floor, and the other is outerbox wall of the operating floor. Both models are single degree of freedom inelastic systems defined by

equivalent shear stiffness and lumped mass. Inelastic relationship between forces and deformations is evaluated according to AIJ code[3] and Technical Guideline for Nuclear Power Plants[4]. Hysteresis characteristic is treated as the degrading tri-linear Takeda model[5] for bending failure structure shown in Figure 1. Damping coefficient c of the system is assumed to be $h = 0.05$.

Figure 2 shows the reinforced concrete column model. Analytical condition is shown as Table 1 where italics indicate the standard condition in analyses. The reinforced concrete wall model for shear failure structure is shown in Figure 3 and Table 2.

2.3 *Input Ground Motions*

One artificial wave and two observed strong ground motions, El-Centro 1940 NS and Taft 1952 EW, are used in inelastic response analyses. Elastic response velocity spectra are shown in Figure 4. Acceleration time histories are shown in Figure 5. For reinforced concrete column model the amplitude of the earthquake motion is proportionally increased to the range μ =5. For reinforced concrete shear resistant wall model, maximum acceleration is taken as 3G.

3. RESULTS

3.1 *Moment Resistant Frame Model*

Results of reinforced concrete column model under artificial wave are as follows. Figure 6 shows the relationship between ductility factor and energy dissipation under the various hysteresis characteristics. Normalized energies(E_H/E_I) reveal great difference between Takeda model and others. Because hysteresis rule of the degrading tri-linear Muto model[6] is similar to that of peak-oriented model before yield, normalized energy(E_H/E_I) is smaller than that of Takeda model. The energy dissipation ratio(E_H/E_I) of Takeda model for the range of large ductility factor is less than that of smaller ductility factor. It is because that damping factor is assumed to be constant and hysteresis response loop is tend to oscillate in one side. Hysteresis model is considered as dominant factor for energy dissipation. Takeda model is used in the following analyses. Figure 7 shows normalized hysteresis energy(E_H/E_{H1}), concerning to the various yield strength of the system, where E_{H1} is the hysteresis energy for μ =1. There is a good agreement with one another. To investigate the effect of the natural period of structure(T_0), three difference models which have same analytical condition without mass are analyzed. As shown in Figure 8, the relationships between input energy and hysteresis energy are similar. It is observed that for the large damping factor the smaller ratio of E_H/E_I, in Figure 9.

Comparison of energy dissipation under three difference strong motions, one artificial wave and two observed strong ground motions, is carried out. The relationship between hysteresis energy dissipation and magnitude of earthquake motion is shown in Figure 10.

Although earthquakes have different characteristics, similar tendency is obtained that the energy dissipated by the structure is getting greater according to the increase of input motion magnitude.

3.2 *Shear Resistant Wall*

Nonlinear characteristic of shear resistant wall structure in the turbine building is surveyed as follows. Shear resistant wall is subjected to combined shear and bending. In this study, shear wall is treated as an equivalent shear model, after comparing the responses of an equivalent shear model with those of a shear bending model. Analytical conditions and obtained responses of the two models are shown in Table 3. Because there are few differences between those responses, it might be able to assume that hysteresis characteristic of an equivalence shear model is Takeda model for the preliminary analysis. Yield strength and yield deformation of shear resistant wall model are adjusted by multiplying the factor α, where α is in the range of 0.3 to 1.5.

Three strong input motions are used in following analyses. Figure 11 shows energy response of shear resistant wall for various input motions. It can be confirmed by hysteresis responses shown in Figure 12 that artificial wave have large input energy than others. The energy dissipation and ductility factor relationship is shown in Figure 13. These figures indicate the tendency that the energy dissipated by the structure is getting larger proportionally according to the increase of ductility factor. As shown in Figure 14, the ratio of energy dissipation is stable in all range of ductility factor for any input motion in the case of Takeda hysteresis model. Figure 15 shows the relationship between ductility factor and reducing strength factor α. Ductility factor seems to have a close relationship with reducing strength factor. In Figure 16, the relationship between energy factor normalized by μ_{e1} and ductility factor is shown, where μ_{e1} is the energy factor for μ=1. Linear correlation of energy factor and ductility factor can be observed for each earthquake.

Further research is executed concerning to momentary input energy. Figure 17 shows the time history of momentary input energy $\Delta E/\Delta t$ and drift angle γ during earthquake. Peak response of drift angle and large momentary input energy seem to be occurred at almost same time. This means that large momentary input energy(ΔE) causes damage of the structure.

4. CONCLUSION

The energy dissipated by the turbine building during earthquake is investigated. The conclusions based on this study are as follows. For the energy dissipated by the structure, hysteresis model is considered as the most dominant factor. Input motion of the earthquake, yield stress of the component, natural period of the structure and damping factor make slight difference in the response values, if the energy values are normalized

by energy or strength for yield point. Ductility factor seems to have a close relationship with hysteresis energy corresponding to the specified hysteresis characteristics. Furthermore momentary input energy may be able to indicate nonlinearity of the system. Energy factor(μ_e) and momentary input energy(ΔE) could be applied to estimate damage of the turbine building as well as ductility factor.

5. REFERENCES

1. Akiyama, H. 1985. *Earthquake-Resistant Limit-State Design for Buildings*, University of Tokyo Press.
2. Nakamura,T., Hori,N., Inoue,N. and Shibata,A. 1996. A Study on Response and Damaging Potential of Hyogoken-Nanbu Earthquake using Observed Ground Motion Records. Department of Architecture, Tohoku University.
3. AIJ. 1988. *Standard for Structure Calculation of Reinforced Concrete Structures.* Architectural Institute of Japan.
4. JEAG 4601-1991. *Technical Guidelines for Aseismic Design of Nuclear Power Plants Supplement.* Japan Electric Association.
5. Takeda, T., M. A. Sozen and Neilson, N. N. 1970. Reinforced concrete Response to Simulated earthquake. *Journal of Structure Division, ASME, Vol.96, No.ST12.*
6. Muto,K., Uchida,T., Tutagawa,T. and Honma,S. 1978. Structure Test and Analysis on the Seismic Behavior of the Reinforced Concrete Reactor Building. *Trans. of Architectural Institute of Japan, No.271.*

Table 1(a) Analytical Parameters of Moment Resistant Frame Model

Parameters	(1)	(2)	(3)
Hysteresis Model	peak-oriented	Muto	*Takeda*
Input Motion	El-Centro	Taft	*Artificial Wave*
Yield Strength	45tf	*90tf*	125tf
Natural Period	*0.5s*	1.0s	2.0s
Damping	0%	*5%*	10%

Table 1(b) Moment Resistant Frame Model (α=1.0)

Items	γ (rad)	Q (tf)
Cracked Strength	0.0014	35
Yield Strength	0.012	90
Ultimate Strength	0.240	90

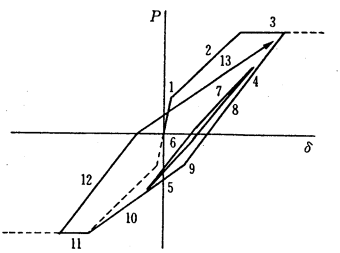

Figure 1 Hysteresis Model of Takeda Model

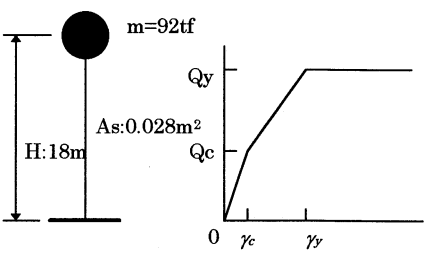

(a) model (b) skeleton curve

Figure 2 Moment Resistant Frame Model

Table 2 Shear Resistant Wall Model

	Items	γ(rad)	Q(tf)
Shear	Cracked Strength	0.18×10^{-3}	1690
	Yield Strength	0.54×10^{-3}	2280
	Ultimate Strength	4.00×10^{-3}	4490
	Items	φ(rad/m)	M(tf·m)
Bending	Cracked Strength	8.8×10^{-6}	22000
	Yield Strength	38.5×10^{-6}	62600

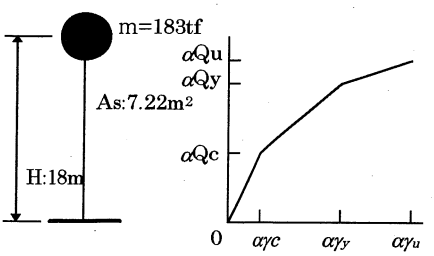

(a) model (b) skeleton curve

Figure 3 Shear Resistant Wall Model

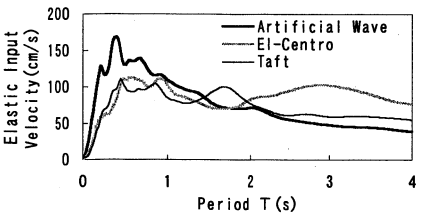

Figure 4 Elastic Response Velocity Spectra
(Maximum acceleration 2.7m/s², h=0.05)

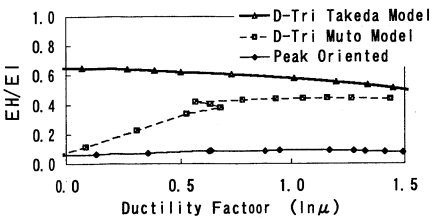

Input Motion : Artificial wave

Figure 6 Comparison of Energy Dissipation Ratio(E_H/E_I) for Three Types Hysteresis Models

Table 3 Comparison of Equivalent Shear Model with Shear Bending Model(α=0.7)

Items		Equivalent Shear Model	Shear Bending Model
Shear	As	7.22m²	10.35m²
Hysteresis Model		Takeda	Peak-Oriented
Bending	I	–	1187m⁴
Hysteresis Model		–	Takeda
Damping Factor		5.0%	5.0%
Acceleration		39.1m/s²	42.7m/s²
Drift		1.52cm	1.70cm
Shear Force		188tf	179tf

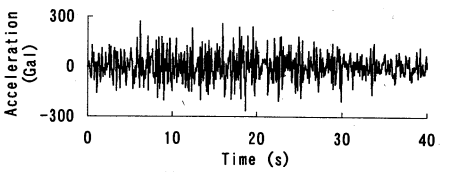

(a) Artificial wave

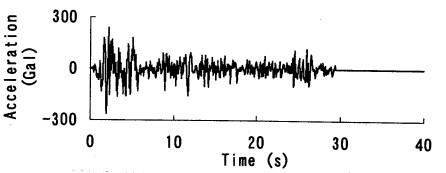

(b) El-Centro 1940 NS

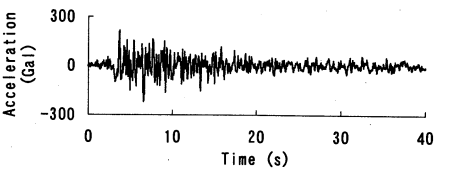

(c) Taft 1954 EW

Figure 5 Input Motion Time History
(Maximum acceleration 2.7m/s²)

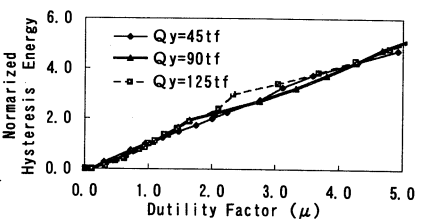

Input Motion : Artificial wave
Hysteresis model : Takeda

Figure 7 Comparison of Normalized Hysteresis Energy(E_H/E_{H1}) for yield strength

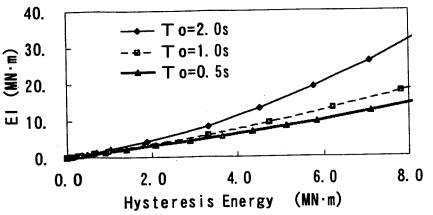

Input Motion : Artificial wave
Hysteresis model : Takeda

Figure 8 Comparison of Input Energy(E_I) for there Types Natural Period System

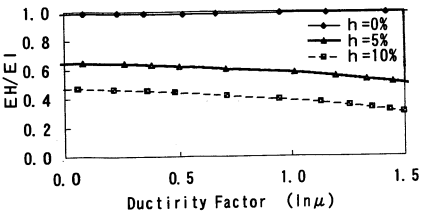

Input Motion : Artificial wave
Hysteresis model : Takeda

Figure 9 Comparison of Energy Dissipation Ratio(E_H/E_I) for Damping Factor

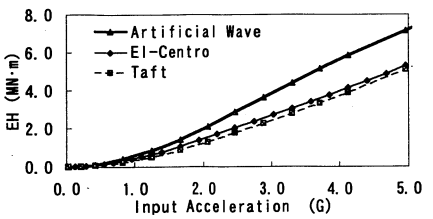

Hysteresis model : Takeda

Figure 10 Comparison of Hysteresis Energy (E_H) for Strong Input Motions

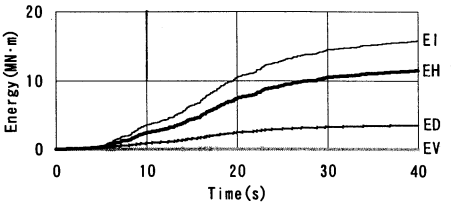

(a) Artificial Wave

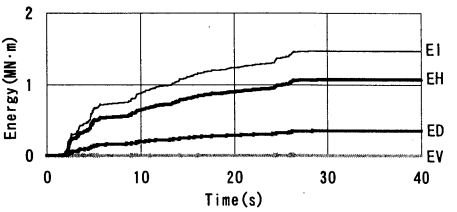

(b) El-Centro 1940 NS

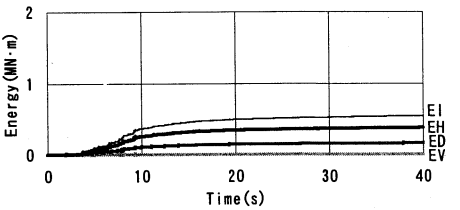

(c) Taft 1952 EW

Input Motion : 3G
Hysteresis model : Takeda

Figure 11 Energy Response(α=0.7)

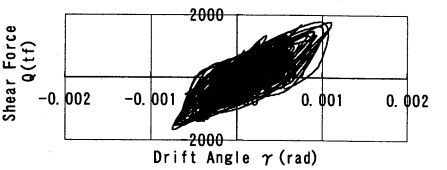

(a) Artificial Wave

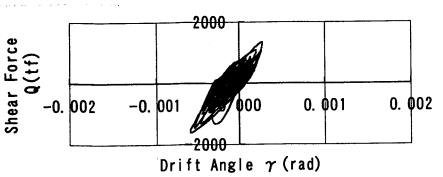

(b) El-Centro 1940 NS

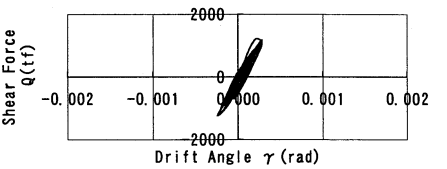

(c) Taft 1952 EW

Input Motion : 3G
Hysteresis model : Takeda

Figure 12 Hysteresis Response(α=0.7)

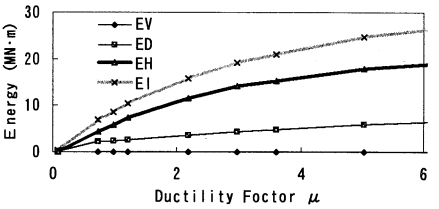

(a) Artificial Wave

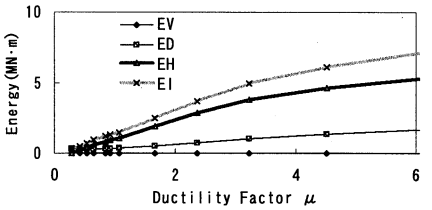

(b) El-Centro 1940 NS

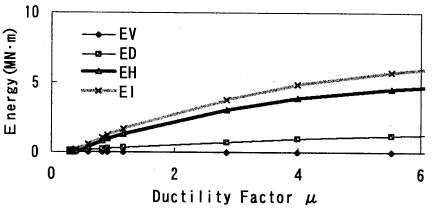

(c) Taft 1952 EW

Input Motion : 3G
Hysteresis model : Takeda

Figure 13 Energy Dissipation and Ductility Factor(μ) Relationship

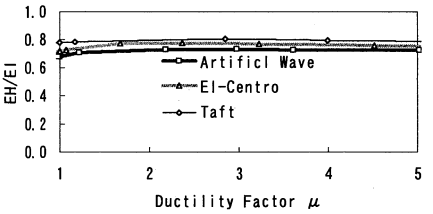

Input Motion : 3G
Hysteresis model : Takeda

Figure 14 Comparison of Energy Dissipation Ratio(E_H/E_I) for Strong Input Motion

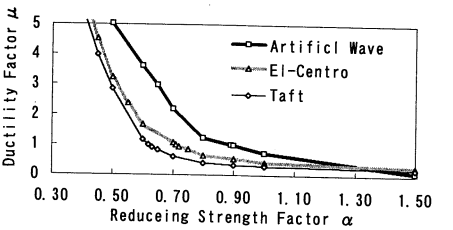

Input Motion : 3G
Hysteresis model : Takeda

Figure 15 Ductility Factor (μ) and Reducing Strength Factor(α) Relationship

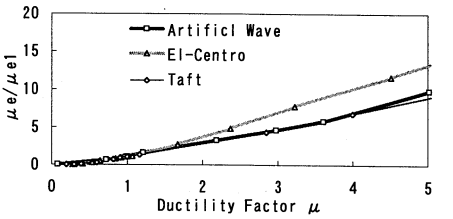

Input Motion : 3G
Hysteresis model : Takeda

Figure 16 Normalized Energy Ductility (μ_e/μ_{e1}) and Ductility Factor(μ) Relationship

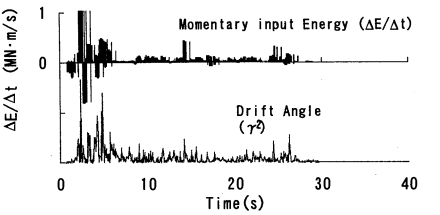

Hysteresis model : Takeda

Figure 17 Momentary Input Energy $\Delta E/\Delta t$ and Drift Angle (α=0.7,El-Centro 3G)